



NTNU – Trondheim
Norwegian University of
Science and Technology

DISCONNECTION OF WORKOVER RISERS ON VERY DEEP WATER

Benjamin Ingvaldsen Brynestad

Marine Technology

Submission date: June 2012

Supervisor: Carl Martin Larsen, IMT

Co-supervisor: Øystein Wærstad, Aker Solutions

Norwegian University of Science and Technology
Department of Marine Technology



NTNU Trondheim
Norwegian University of Science and Technology
Faculty of Engineering Science and Technology
Department of Marine Technology

M.Sc. thesis 2012

for

Stud. tech. Benjamin Brynestad

DISCONNECTION OF WORKOVER RISERS ON VERY DEEP WATER

(Frikobling av stigerør for brønnvedlikehold på stort vanddyb)

Drilling and well intervention on very deep water require high quality analyses of the marine riser for a set of conditions. Analyses are needed to assist riser installation and disconnection operation as well as classical analyses of a connected riser under varying current and wave conditions. The present project should focus on disconnection of workover risers under varying operational and environmental conditions. Unexpected drift-off or drive-off should in particular be included. Modelling aspects of the entire riser system including the heave compensator should also be addressed.

In order to investigate riser operations in stochastic waves one may need to carry out a large number of analyses. This will require use of software that can change input, initiate batch computations and store key output from programs like RIFLEX. Programming and use of this type of software should be a part of the present project.

The work should be carried out in steps as follows:

1. Literature study, including workover riser technology and operations, modelling of riser systems for dynamic analysis, and software for organising sequences of analyses. Topics that were addressed in the pre-project need not to be repeated in this work.
2. Select a typical workover riser for deep water operations (3-4000 meters), and make alternative RIFLEX models of this riser with varying complexity.
3. Describe actual operations related to well intervention, and analyses that are needed in order to ensure safe operations. Recoil operations should in particular be described.
4. Apply RIFLEX to carry out a set of analyses for investigation of interesting aspects of riser disconnection under a variety of environmental and operational conditions. The cases to be analysed should be agreed with the supervisor.

The work may show to be more extensive than anticipated. Some topics may therefore be left out after discussion with the supervisor without any negative influence on the grading.

The candidate should in her/his report give a personal contribution to the solution of the problem formulated in this text. All assumptions and conclusions must be supported by mathematical models and/or references to physical effects in a logical manner.

The candidate should apply all available sources to find relevant literature and information on the actual problem.

The report should be well organised and give a clear presentation of the work and all conclusions. It is important that the text is well written and that tables and figures are used to support the verbal presentation. The report should be complete, but still as short as possible.

The final report must contain this text, an acknowledgement, summary, main body, conclusions and suggestions for further work, symbol list, references and appendices. All figures, tables and equations must be identified by numbers. References should be given by author name and year in the text, and presented alphabetically by name in the reference list. The report must be submitted in two copies unless otherwise has been agreed with the supervisor.

The supervisor may require that the candidate should give a written plan that describes the progress of the work after having received this text. The plan may contain a table of content for the report and also assumed use of computer resources.

From the report it should be possible to identify the work carried out by the candidate and what has been found in the available literature. It is important to give references to the original source for theories and experimental results.

The report must be signed by the candidate, include this text, appear as a paperback, and - if needed - have a separate enclosure (binder, DVD/ CD) with additional material.

Supervisor at NTNU is professor Carl M. Larsen

Trondheim, 16. January 2012

Carl M. Larsen

Submitted: 16. January 2012

Deadline: 15. June 2012

Abstract

As oil recovery is moving too deeper and deeper water there is an increasing demand for advanced riser analysis. Deep water oil recovery have forced a change in the systems used to tension risers, the traditional wire-pulley systems are replaced with direct acting hydraulic-pneumatic systems. In order to design these systems to obtain the desired operability, analysis tools including the heave compensation system is necessary. As a result a pipe in pipe RIFLEX model have been developed.

In this masters thesis the pipe in pipe model will be used to investigate drive-off and weak link fracture. Both subjects investigated exposes the riser to large forces, and will push the model to its limits. Another part of the thesis is focused around batch execution of analyses with the use of MATLAB.

The focus of the drive-off study lies mainly in investigating the dynamic behaviour of a deep water riser (3000[m] water depth) compared to a shallow water riser (300[m] water depth). Results are presented for upstream and downstream drive off scenarios. The maximum offset is 100[m] obtained during a 50[s] period. Drive-off scenarios include cases where the vessel remains at the 100[m] offset, and cases where the vessel returns to its original position.

Drive-off simulations revealed large differences in dynamic behaviour of the deep water versus the shallow water system. When observing the lower riser angle for shallow water simulations, the angle were closely related to the vessel offset position. Deep water simulations showed a delay of almost one minute before the lower angle responded with a rotation in the vessels movement direction. During the first minute an initial effect that caused the riser to rotate away from the vessel position was observed. Current had a limiting effect on the lower angle when driving upstream, and increased the angle for downstream drive-off. By including a return motion the riser angle increased more rapidly to large values. Variation in return motion had little effect on the maximum amplitude. The results show that it might be difficult to take advantage of the dynamic delay in the riser response. Bear in mind that offsets of only 100[m] was investigated, the picture might change for simulations including larger vessel offset.

Weak link fracture is of concern since it will release large amounts of stored energy that is potentially harmful for personnel and equipment. Establishing analysis

methods for weak link fracture can help to better understand the dynamics of the problem. In the present work a suitable analysis model was selected and a parametric study on the effect of drag on response was performed.

A weak link fracture was simulated with 460 tonnes over pull. Weak link fractures is a highly complex problem since the high pressure content of the riser is released into the water, causing a rocket effect. The presented results are only accounting for potential energy stored as strain in the riser and heave compensation system. A parametric study of the tangential drag versus the maximum vertical amplitude of the riser is presented. The results are meant to be used as a starting point in an investigation of measures to limit the weak link fracture response.

The weak link simulations showed that large accelerations are involved during the weak link fracture, and therefore added mass and mass can be of importance to the response. Due to the rapid movement after fracture, it was found that special care needs to be taken when selecting the time incrementation for the simulations.

Preface

The interest for riser analysis was triggered during a summer intern ship with Aker Solutions where I worked with problems related to well-head modelling in a global riser analysis. During the pre-project for this thesis I studied modelling of riser disconnection on a simple model. In the presented work I got to work with a more complex model including the heave compensator system. An unexpected amount of time went into solving numerical problems with the model, but left me with valuable experience I believe is easily transferable into a work environment.

This master's thesis has been supervised by professor Carl M. Larsen. Input data and practical input has been provided by Aker Solutions, via Øystein Wærstad and Ronny Sten.

I would like to thank my academical advisor, Carl M. Larsen for good support and availability through the process. I would also like to express my gratitude towards Philippe Maincon for providing me with support and information on how to run batch analysis.

In addition I would like to thank Øystein Wærstad and Ronny Sten from Aker Solutions for providing insight and relevant input data from the industry.

Benjamin I. Brynestad

Trondheim, June 8, 2012

Contents

Abstract	v
Preface	vii
List of Figures	xi
List of Tables	xiii
1 Introduction	3
1.1 Drive-off	3
1.2 Weak link fracture	4
1.3 Compensation systems	4
2 Batch programming	7
3 Analysis	9
3.1 Heave compensation	9
3.1.1 Constant force model	9
3.1.2 Time varying force model	10
3.1.3 Pipe in pipe model	10
3.2 Calculation of lower riser angle	14
3.3 Damping	14
3.4 Drive-off	15
3.4.1 RIFLEX models	16
3.4.2 Vessel drive-off motion	19
3.4.3 Current	19
3.4.4 Analysis methodology	20
3.5 Weak Link	20
3.5.1 Tangential drag	21
3.5.2 Analysis methodology	21
3.5.3 Parametric variation	23
3.5.4 Riflex model	23
4 Results	25
4.1 Drive-off	25
4.1.1 Riser snapshots	25

4.1.2 Lower angle of the riser	28
4.2 Weak link fracture	34
5 Conclusion	39
6 Further work	41
6.1 Drive-off	41
6.2 Weak link fracture	41
References	I
Appendix	I
A Matlab script for calculation of global angle	III
B Matlab script for calculation of relative angle	V
C geninp.m	VII
D reflex_test.m	IX
E replaceinfile.m	XI
F Matlab functions used for post processing drive off	XIII
G Matlab function used to convert ascii files to mat	XVII
H Matlab functions used to generate drive off	XIX
I Matlab function used to tune tension	XXIII

List of Figures

1.1	Heave compensator systems	5
1.2	Hydraulic-pneumatic heave compensator.	5
3.1	Constant force heave compensator model	10
3.2	Contact forces	11
3.3	Positioning of tensioning spring in a single heave compensation cylinder.	12
3.4	Heave compensator spring properties	12
3.5	Exploded view of alternative RIFLEX models for a single heave compensator cylinder.	13
3.6	Damping ratio vs frequency	15
3.7	TSJ profile.	16
3.8	Model used for drive-off analysis in deep water.	17
3.9	Model used for drive-off analysis in shallow water.	18
3.10	Drive-off signal for various scenarios	19
3.11	Current profiles	20
3.12	Effective tension at the weak link versus vessel offset.	22
3.13	Effective tension at the weak link versus vessel offset.	23
3.14	Time series of lower end vertical movement	23
3.15	Model used for weak link analysis.	24
4.1	Deep water time snapshots, 50 [s] 100[m] drive-off no current.	26
4.2	Shallow water time snapshots, 50 [s] 100[m] downstream drive-off no current.	26
4.3	Deep water time snapshots, 50 [s] 100[m] downstream drive-off shear current.	27
4.4	Deep water time snapshots, 50 [s] 100[m] upstream drive-off shear current.	27
4.5	Shallow water time snapshots, 50 [s] 100[m] drive-off shear current.	28
4.6	Lower angle during downstream drive-off with shallow water configuration.	29
4.7	Lower angle during upstream drive-off with shallow water configuration.	29

4.8	Lower angle during downstream drive-off with deep water configuration.	30
4.9	Lower angle during upstream drive-off with deep water configuration.	31
4.10	Deep water lower angle comparison during downstream drive-off to 100[m] offset in 50 [s].	31
4.11	Study of return motion on deep water riser with downstream vessel motion.	32
4.12	Study of return motion on deep water riser with upstream vessel motion.	33
4.13	Lower angle during upstream drive-off with deep water configuration using the tensioned spring model.	34
4.14	Motion of the lower end of the riser after weak link fracture.	35
4.15	Parameter study of weak link fracture.	36
4.16	Vertical displacement, velocity and acceleration for lower end, $cd = 0$	36
4.17	Vertical displacement, velocity and acceleration for lower end, $cd = 600$	37
4.18	Data points for vertical acceleration.	37

List of Tables

3.1 Initial drive-off load cases	15
--	----

Nomenclature

α_1	Mass proportionality factor.
α_2	Stiffness proportionality factor.
A_d	Amplitude of drive-off motion.
C	Damping matrix.
D_d	Duration of drive-off motion.
D_s	Drive-off start time.
K	Stiffness matrix.
M	Mass matrix.
t	Time variable.
$x_d(t)$	Drive-off position at time t .
$x_r(t)$	Return position at time t .
AKSO	Aker Solutions
ASCII	American Standard Code for Information Interchange.
DYNAMOD	Dynamic module in reflex.
EDP	Emergency disconnect package
FE	Finite elements.
HP	High pressure
LP	Low pressure
LRP	Lower Riser Package
LRP	Lower riser package.
MATLAB	Numerical computing environment and fourth-generation programming language.
OMAE	International Conference on Ocean, Offshore and Arctic Engineering

STAMOD Static module in reflex.

TSJ Tapered stress joint

WH Wellhead

XT X-mas tree

Chapter 1

Introduction

The aim for this paper is to investigate riser response during drive-off scenarios, and to study the riser response during weak link fracture.

Two different riser configurations will be analysed, and compared. The first configuration is a workover riser for operation in shallow waters at 300 metres water depth. The second configuration is a riser configured for operation at 3000 metres water depth. From now on the two configurations are referenced to as shallow water and deep water.

1.1 Drive-off

Drive-off is an event where control over the DP-system is lost, resulting in an uncontrolled excursion of the vessel. This uncontrolled movement can lead to critical failure and damage to people and environment. When establishing operating envelopes the lower riser angle is of concern since it limits the window where a controlled disconnect can be executed. Monitoring of the top angle is also important to avoid collision between riser and vessel. Results presented does not include top angles due to limitations in the analysis method. By studying the behaviour of the lower angle during drive-off one can obtain a better understanding of the effects that occur during drive-off. This knowledge can lead to larger operation envelopes and safer operation.

In [Ervik, 2011] and [Rustad et al., 2012] it was found that large dynamic effects take place, especially on deep water risers. A significant delay of 35[s] was observed on the response of the lower riser angle for a 2000 [m] riser configuration. Additionally it was found that the current have a large effect on the lower angle. When driving off upstream the current prevented large angle amplitudes. During downstream drive off application of current increased the angle amplitudes.

In the present work effect of vessel return is included, and a pipe in pipe heave compensator model is used in the analyses. The pipe in pipe model probably affects the lower angle to a limited degree, but was used to test the model and familiarize with it.

1.2 Weak link fracture

Weak link fracture is a possible outcome of an uncontrolled drive-off. A weak link is a part of the riser designed to fail as a last barrier preventing damage to the wellhead and subsea structures. A weak link fracture involves release of high amounts of energy which is of potential danger for personnel and equipment, it should therefore be avoided at all cost. By establishing analysis methods to study the phenomenon, measures can be taken in order to limit the danger involved in the event of a weak link fracture.

During a weak link fracture the pressurized content of the riser is released into the environment. The pressure release cause a rocket effect and may amplify the riser response. This effect would be very demanding and require a multidisciplinary collaboration to investigate. It is therefore beyond the scope of the presented work and neglected in the analyses.

Riser dynamics during a weak link fracture at 460 tonnes over-pull is studied. The analysis includes release of the potential energy stored as elastic strain in the riser and heave compensation system. By incrementally increasing the tangential drag of the lower end of the riser, a parametric study of the maximum vertical riser response versus drag coefficient is performed. The intention is that this study can be used as a basis in a future study investigating possibilities for limiting the riser response.

1.3 Heave compensation systems

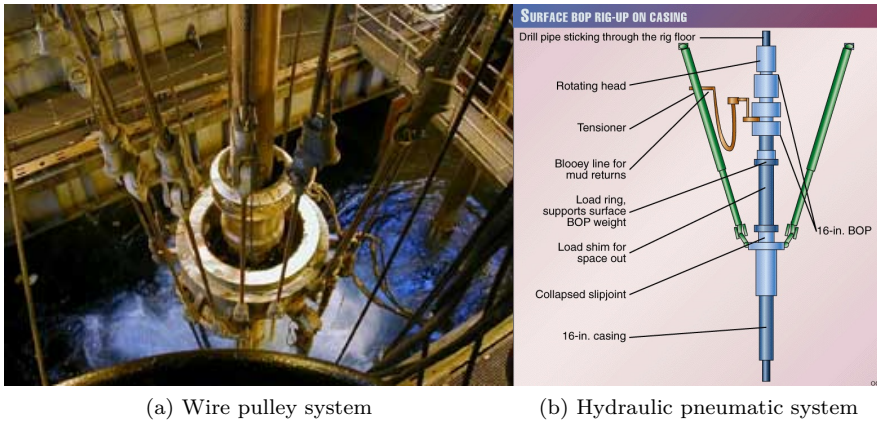
Basic knowledge of heave compensation systems is required in order to understand the motivation for the pipe in pipe model described in section 3.1.3.

Heave compensation systems are required in order to keep the lateral stiffness and tension in the riser at desirable levels. If the tensioning system should fail, large moments will occur at the wellhead, possibly causing a blow-out. The top-tension should be kept at a near constant level especially for deep water risers, as the sensitivity to top tension increases with riser length.

The first riser heave compensators were based on wire and pulley systems. Figure 1.1a displays the connection of a wire pulley system to a riser. As oil recovery moved to deeper and deeper water, the demands on the tensioning systems increased. Resulting in traditional systems being replaced by more advanced,

pneumatic-hydraulic systems with direct-acting pistons. Wear and tear of these systems have proved to be undesirably high, therefore better analysis tools to improve design are of growing concern. The pipe in pipe model used in the presented work is a result of this development. It can be used to better understand the moment and force distributions over the hydraulic cylinders.

Figure 1.1b illustrates how a pneumatic-hydraulic system is connected to the riser. A system schematic is illustrated in Figure 1.2. The low pressure(LP) side of the cylinder prevents the rod head from bottoming out, while the high pressure (HP) side of the system provides the tensioning properties of the system. By adjusting the pressure in the high pressure vessel tensioning can be controlled in a better way than with wire-pulley systems. Hydraulic fluid is used to transfer the pressure to the rod head.



(a) Wire pulley system

(b) Hydraulic pneumatic system

Figure 1.1: Heave compensator systems

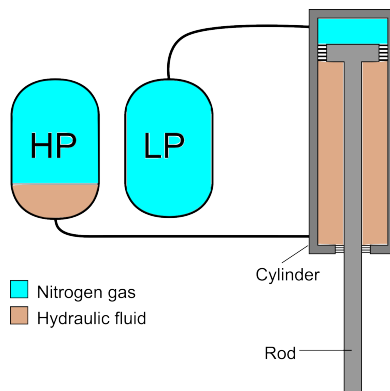


Figure 1.2: Hydraulic-pneumatic heave compensator.

Chapter 2

Batch programming

In order to run series of analyses efficiently batches of RIFLEX analyses was executed using MATLAB.

To change variables and organise the analyses in an efficient manner, the script “geninp.m” was programmed. It replaces variables in an input file and places the modified input files in folders based on case names. “geninp.m” is a function, and can therefore easily be implemented in larger programs. To replace variables in the RIFLEX input file, “geninp.m” calls the function “replaceinfile.m” which is a script that can be found at the MATLAB central [mat, 2011]. The script is included in appendix E.

Below is an example of what the input file for “geninp.m” looks like. Line one lists the different variable names and column one lists the case names. The three variables are named “V_DDUR”, “V_DAMP” and “V_RDUR” and the case-names are “50_S_100M_200SR” and “50S_100M_300SR”. A new row is started with a return, columns are separated using tab

```
1 Cases      V_DDUR  V_DAMP  V_RDUR
2 50S_100M_200SR  50  100  200
3 50S_100M_300SR  50  100  300
```

“replaceinfile.m” then searches the RIFLEX input file for the variable names and replaces them with the values listed. “geninp.m” then places the modified file in a folder named after the case. The relevant part of the RIFLEX input file is shown below. On line 3 the variable names is replaced, enabling RIFLEX to use the correct “.txt” file during analysis. The code for “geninp.m” is included in appendix C.

```
1 WFMOTION TIME SERIES
2 'ives chftsf                iform ikind irot icotim icoxg icoyg ...
   icozg icoxgr icoygr icozgr
```

```

3  1  V_DDURs_driveoff_to_V_DAMPm_V_RDURs_return.txt ASCII DYND ...
    DEGR 1      2      3      4

```

When the file and folder structure is established the analyses can be run. The function “riflex_test.m” included in appendix D. executes the riflex analysis and echoes the dos output to matlab.

“riflex_test.” executes “riflex.bat” with extra parameters defining analysis type and input files. For instance the command “riflex.bat stamod 300m_riser” would run a static analysis with the STAMOD module using the input file “300m_riser_stamod.inp”. This operation is performed using the MATLAB dos command as shown in line two in the code below. As an additional option “-echo” outputs the text usually displayed in the dos command window to the MATLAB command window. The variable ”bat” is a string containing the location to the riflex.bat file, “pref1” is a string containing the prefix of the stamod input file. (e.g. 206m_PIP_alle_mod)

```

1  cmd = [bat ' stamod '      pref1      ];
2  status = dos(cmd, '-echo');  assert(~status, 'DOS reported an error');

```

In the present work the main effort is studying riser dynamics, most of the results is therefore based on the position of the riser. A print option for printing out nodal positions of the riser is enabled in the DYNMOD input files. Output is given as ASCII files, which are easy but slow to load into MATLAB. Therefore the ASCII files is converted into mat files, which is much faster to load. Conversion is done using the function “convert_timeseries_to_mat.m” included in appendix G. The same input file that was used to generate the load cases is used to locate the ASCII files and correctly name the mat files. Converted data is gathered and stored in a folder named “Matlab_time_series”.

Chapter 3

Analysis methodology

This chapter contains a description of the models and analysis methods used to produce the results. All analyses were carried out using RIFLEX version 3.7.24. RIFLEX is a well known industry standard beam based FE-program. It is suitable for static and dynamic analysis of slender structures. Version 3.7.24 is an internal version, it is therefore not certain that the presented functionality is commercially available at the present date.

3.1 Heave compensation system modelling

A brief introduction to heave compensation systems is found in chapter 1.3. In the following different methods for modelling of heave compensation systems is presented and discussed.

3.1.1 Constant force model

The simplest way to model a heave compensation system is to apply a constant vertical force in the top of the riser while horizontal movement is connected to the vessel. Force variations in the tensioning system cannot be represented in this model. These force variations will mainly affect the upper parts of the riser and be damped out with increasing water depth. This model would be sufficient for the drive-off analyses since the parameter studied is the lower angle of the riser, which is located close to the seabed. For weak link fracture analysis the model is insufficient, since the lower end of the riser is free after the fracture, enabling the constant force to pull the riser out of the water. Figure 3.1 gives an illustration of the constant force model.

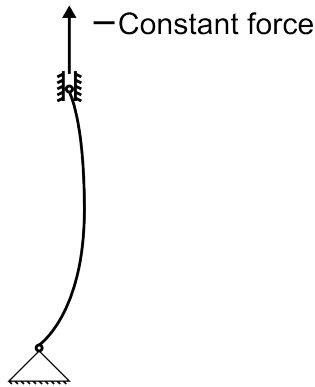


Figure 3.1: Constant force heave compensator model

3.1.2 Time varying force model

A more advanced approach would be to replace the constant force with a time varying force based on simulations of the tensioning system. The time variation of the force is estimated by simulating the heave compensation system in a separate simulation program based on vessel movement, and then implementing it in the RIFLEX model. This approach would also cause issues when releasing the lower end of the riser.

3.1.3 Pipe in pipe model

The pipe in pipe model used in the analyses were provided by Aker Solutions via Ronny Sten. It was originally used to investigate bending moments and forces on the heave compensator systems cylinders and rods.

In the PIP model the hydraulic heave compensation system is represented by elements with pipe cross-sections with contact formulation. The pressure bank properties is represented by a circular cross-section acting as a spring.

This is the model used in the analyses since it was the only solution allowing representation of the top tension system after disconnection of the lower end. The model was also used in the drive-off analyses in order to obtain additional experience with the PIP modelling.

Contact forces

Contact is modelled using the pipe in pipe contact formulation implemented in RIFLEX. The contact formulation is searching for contact between tubular contact components, if contact is detected, springs are applied in order to simulate the

contact force. [Rif, 2010] Contact forces in the heave compensator occurs as a result of contact between the rod head and the inner wall of the cylinder, and between the cylinder-end and the rod. The distance between the contact forces can vary dynamically as the rod moves in the cylinder. Figure 3.2 gives a simple illustration of how the contact forces occur.

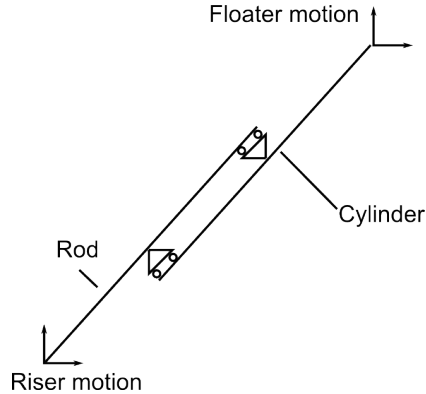


Figure 3.2: Contact forces

Tensioning properties

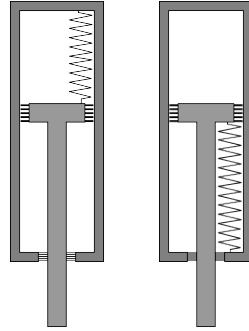
Tensioning properties of the heave compensation system is represented by a spring element. The spring represent the behaviour of the pressure banks connected to the heave compensator cylinders.

Two different configurations for the tensioning spring were used. For the drive-off analysis the spring was connected to the rod head and the bottom of the cylinder. Weak link analysis required large offsets with following high tension in the riser. Resulting in numerical issues due to the compression of the spring elements. As a solution the spring was moved and connected from the top of the cylinder to the top of the rod. Causing the spring to be tensioned instead of compressed. The results show a much more stable system able to handle higher loads. The drawback is that the representations of tension in the cylinder is lost. For the study presented this is not an issue since the moment and forces in the heave compensator is not under consideration. Figure 3.3. illustrates the spring positioning, and should help to visualise why cylinder tension is lost in the model with top a mounted spring. Note that the cylinder rod and spring is modelled as beam elements overlapping each other along a line, the figure serves only for illustrative purposes.

In the subsection presenting the RIFLEX modelling, a model solving the issue with loss of cylinder tension is proposed.

In order to achieve different levels of initial tension a translation of the force-strain curve defining the tension system was needed. To conserve the properties of the

tensioning system, the gradient was kept at a constant level. Figure 3.4 illustrates the superposition for a spring tuned to increase initial tension from 50[kN] to 70[kN].



(a) Weak link (b) Drive-off

Figure 3.3: Positioning of tensioning spring in a single heave compensation cylinder.

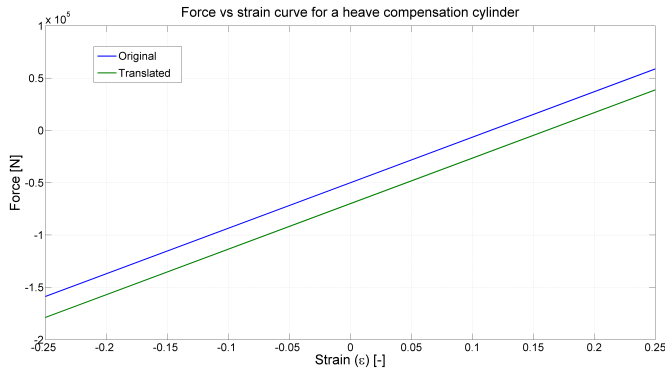


Figure 3.4: Heave compensator spring properties

Riflex modelling

In this section the different RIFLEX models for a single hydraulic heave compensator is presented.

As previously mentioned the cylinder and rod of the tensioner consists of circular cross-sections (CRS1) connected with a spring element with a defined force vs elongation curve. Both the rod line and the cylinder line are segmented, the segments

are used to represent the rod head and the bottom of the cylinder. Contact is then defined between the inner wall of the cylinder and the rod head, and between the rod stem and cylinder bottom.

Connection to the riser is achieved by a set of master slave connections. The lower ends of the piston rods are slaves to the connection node at the riser. The top of the cylinders are linked to the vessels transfer function.

Figure 3.5 shows an exploded view of various RIFLEX models for a single hydraulic tensioner. Differences between the three models lies in the positioning and number of springs used.

Drive-off simulations use a spring mounted under the piston as shown in figure 3.5a. Weak link analysis uses the model with top mounted spring as shown in figure 3.5b. Figure 3.5c shows how numerical stability and force balance in the cylinder can be conserved at the same time by introducing a second spring and a slave node.

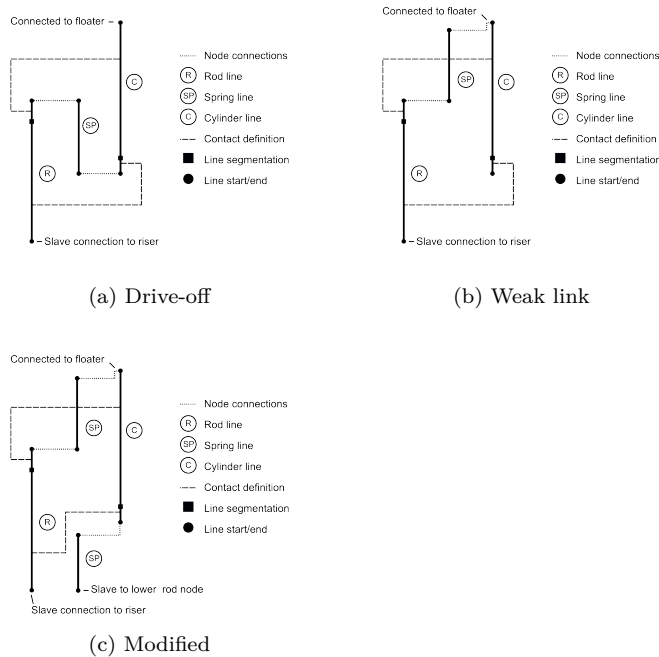


Figure 3.5: Exploded view of alternative RIFLEX models for a single heave compensator cylinder.

Limitations

If the rod head should exit the cylinder during an analysis it is no longer restrained in the lateral direction, and the analysis will most likely fail. Testing showed that

this would not be a likely problem in the present work, but may be an issue for analyses with higher loads. The limitation may for instance be solved by introducing a non-linearity to the tension spring so that the axial force in the springs increases rapidly when the rod head approaches the cylinder ends.

3.2 Calculation of lower riser angle

The studies presented at OMAE 2012 is considering a drilling riser. The lower angle is calculated as the inclination of the elements above and below the balljoint. [Rustad et al., 2012]

The presented work differ from the drilling riser since the workover riser is fitted with a TSJ (Tapered stress joint) instead of a balljoint. Meaning that another method for calculation of the lower angle had to be used. Calculations of the lower angle in the present work is therefore done by trigonometry relations between three nodes. The nodes is located at the top of the TSJ, at the TSJ-EDP interface and at the lower end of the EDP. It is assumed that this method for calculation of the lower angle is adequate. The script “relang.m” is used for calculation of lower riser angle. A positive angle indicate downstream rotation, negative angle indicate upstream rotation. “relang.m” can be found in appendix B.

3.3 Damping

Damping is included using the Rayleigh damping model which is proportional to the mass and stiffness matrix. The formulation is shown in equation 3.1. [Rif, 2010] [Langen and Sigbjörnsson, 1979] The damping coefficient is not straight forward to determine, but if the total damping level for a give frequency is know it is easily calculated. It is however important that analyses with large rigid body motions keep α_1 low to avoid damping of the rigid body modes. In the present work α_1 is set equal to zero, while α_2 is set to 0.115 which leads to the damping ratio to frequency curve shown in figure 3.6.

$$C = \alpha_1 M + \alpha_2 K \quad (3.1)$$

Where:

C is the damping matrix.

M is the mass matrix.

K is the stiffness matrix.

α_1 is the mass proportionality factor.

α_2 is the stiffness proportionality factor.

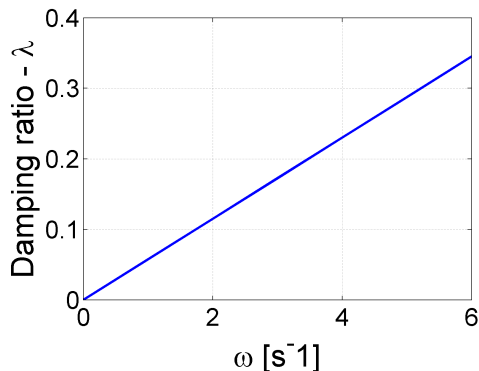


Figure 3.6: Damping ratio vs frequency

3.4 Drive-off

Drive-off simulations were performed for several cases in both deep and shallow water for upstream and downstream motions. The shallow water model is a riser configured for operation at 300 [m] water depth as shown in figure 3.9 , while the deep water version is configured for 3000 [m] as shown in figure 3.8.

Drive-off motion is simulated as a sine squared signal. Figure 3.10 displays drive-off motions for various simulation scenarios. The vessel is moved along the x-axis and current is acting in the positive x-direction.

Wave induced motions is neglected since RIFLEX calculates vessel motions based on transfer functions at the initial position of the vessel. Therefore the vessel motion during drive-off would be based on the wrong position. Additionally the vessel forward speed would alter the vessel motion and the transfer functions provided would be insufficient. Also making monitoring of relative angle between riser and vessel difficult.

Table 3.1 summarise the load cases initially investigated cases for the drive-off scenarios.

	Case 1	Case 2	Case 3	Case 4	Case 5	Case 6
Drive-off amplitude	100[m]	100[m]	100[m]	100[m]	100[m]	100[m]
Drive-off duration	50[m]	50[m]	50[m]	50[m]	50[m]	50[m]
Current	NO	Uniform	Shear	NO	Uniform	Shear
Direction	Upstream	Upstream	Upstream	Downstream	Downstream	Downstream

Table 3.1: Initial drive-off load cases

The drive-off scenarios considered were limited to 50 [s] durations to make the dynamic effects more pronounced. Average vessel speed for the initial load cases is 2 [m/s] and the maximum vessel acceleration is 0.2 [m/s^2].

3.4.1 RIFLEX models

Two RIFLEX models were used for the drive-off simulations, one for each water depth. Both models is based on input provided by AKSO. The data provided is for a system designed for operation at a water depth of 300[m]. Deep water simulations requires that buoyancy elements are added to the riser in order to achieve sufficient tension. The buoyancy modules used in the presented work is the same configuration used in the pre-project, it was selected in order to avoid impact during disconnects. [Brynstad, 2011]

Wellhead stiffness is represented by a lateral and a rotational spring, the spring properties are based on local FE simulations and was provided by AKSO. Figure and figure gives an overview of the two models. The TSJ profile is shown in figure 3.7.

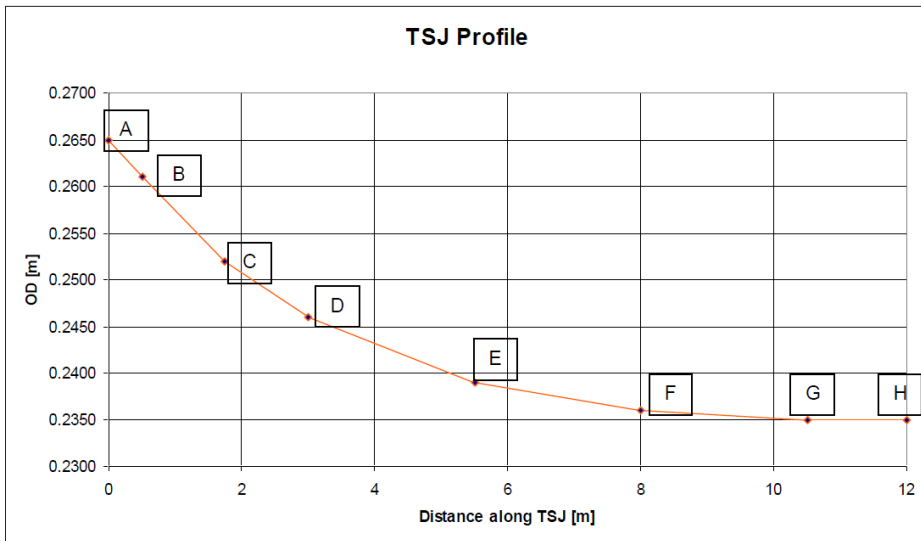


Figure 3.7: TSJ profile.

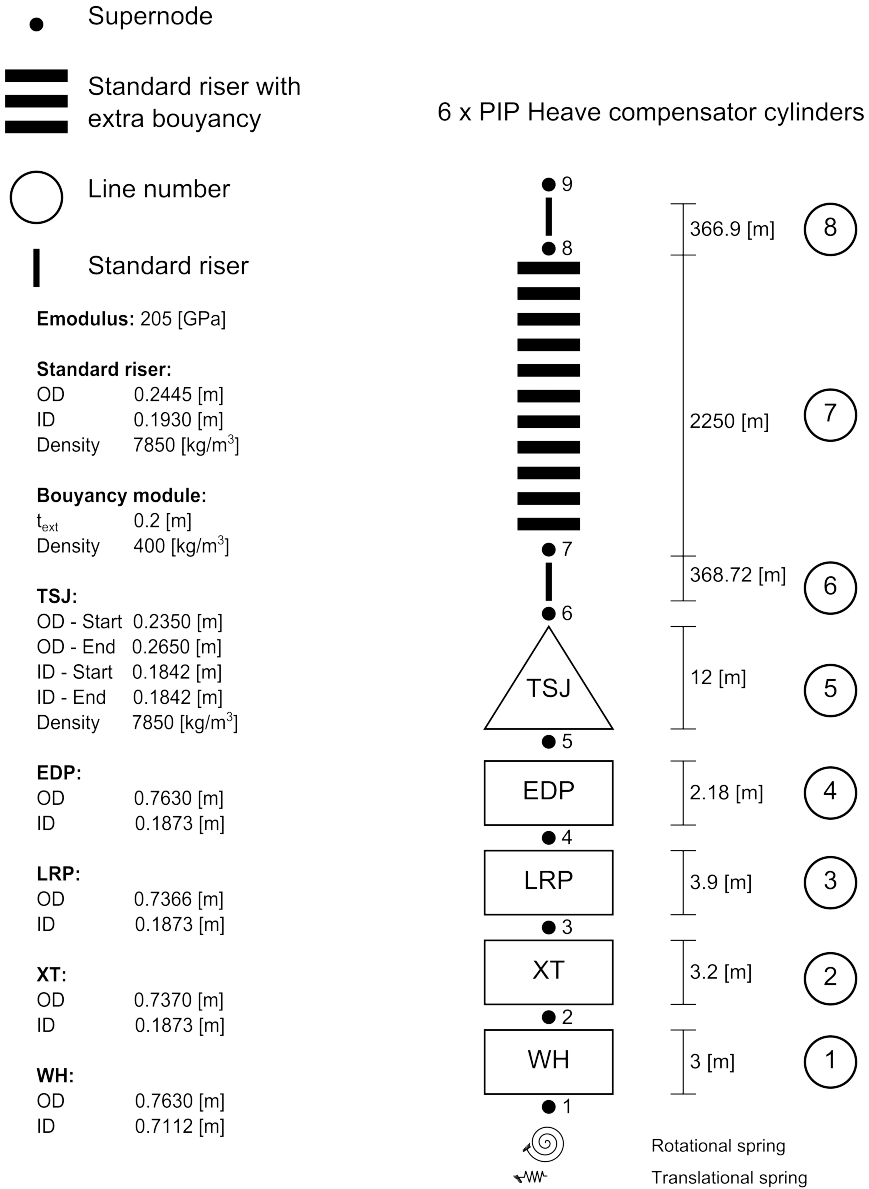


Figure 3.8: Model used for drive-off analysis in deep water.

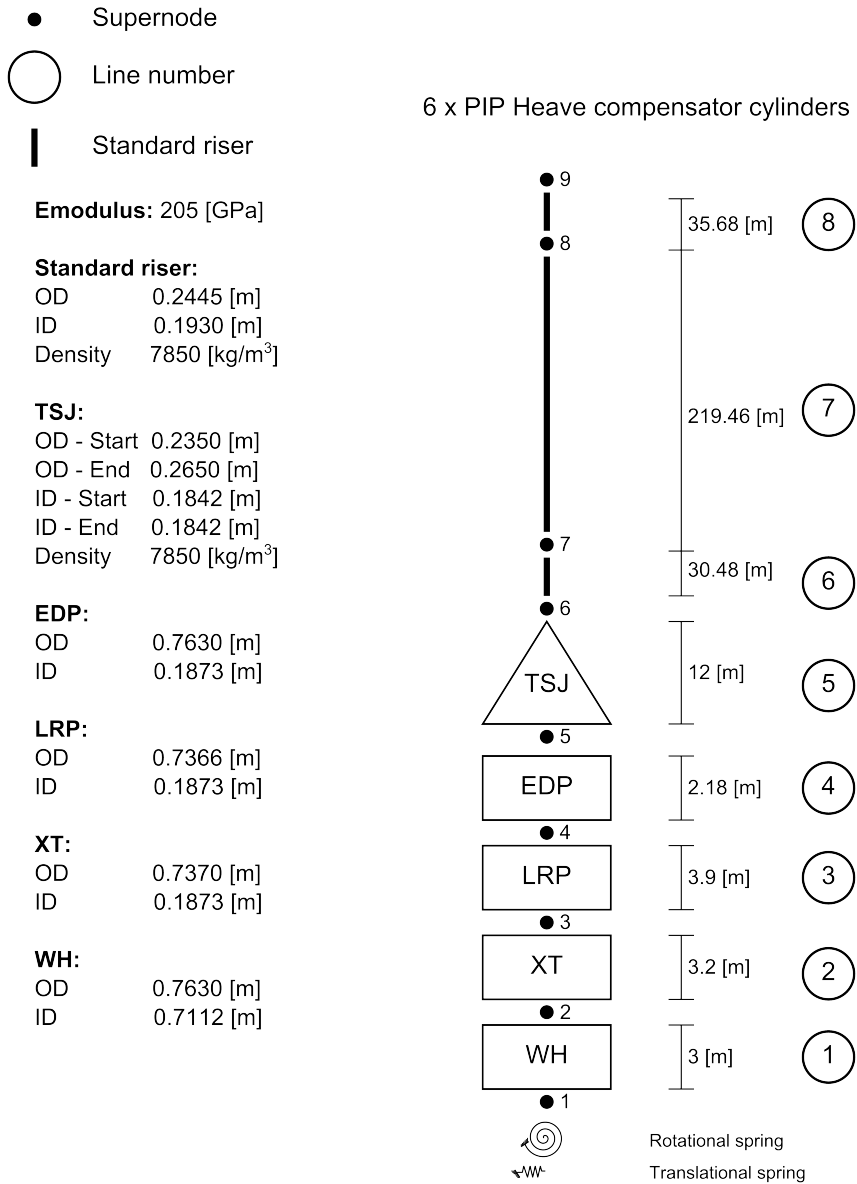


Figure 3.9: Model used for drive-off analysis in shallow water.

3.4.2 Vessel drive-off motion

Vessel drive-off and return motion was simulated based on the trigonometric functions shown in equation 3.2 and equation 3.3. Figure 3.10 illustrates the drive-off motion for various cases. ASCII files was used to implement the motion in the RIFLEX analysis. The files was generated using the code included in appendix H.

$$x_d(t) = A_d \cdot \sin^2\left(\frac{\pi}{2 \cdot D_d}(t - D_s)\right) \quad (3.2)$$

$$x_r(t) = A_d \cdot \cos^2\left(\frac{\pi}{2 \cdot D_r}(t - (D_s + D_d))\right) \quad (3.3)$$

Where:

A_d is the amplitude of the drive-off motion.

D_d is the duration of the drive-off motion.

D_s is the drive-off starting time.

t is the time variable.

$x_d(t)$ is the vessel position during drive-off at time t .

$x_r(t)$ is the vessel position during return at time t .

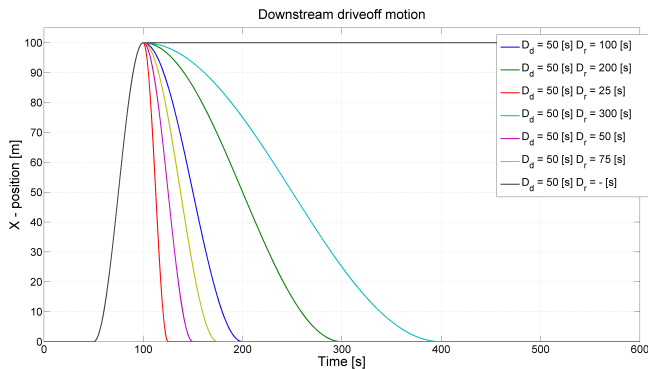


Figure 3.10: Drive-off signal for various scenarios

3.4.3 Current

Two current profiles were investigated, a sheared current and a uniform current. The results for the uniform current on the deep water configuration is not presented

since the large loads caused the analysis to fail. Realistic current profiles are more complex but a sheared current is used for simplicity. If one wishes to investigate more realistic current profiles, the profiles suggested in [Faltinsen, 1990] may be applied. Figure 3.11 illustrates the analysed current profiles.

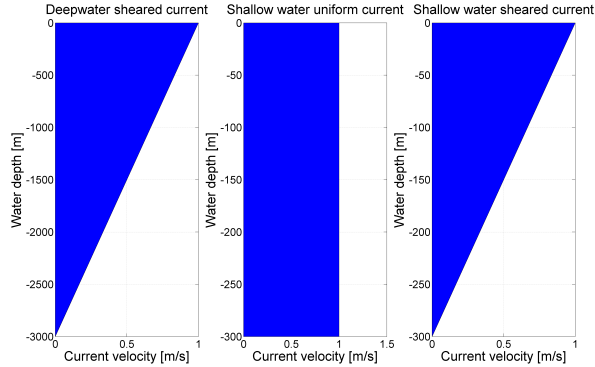


Figure 3.11: Current profiles

3.4.4 Analysis methodology

The analyses were performed using the following procedure:

- Tune over pull at the EDP to a reasonable level by modifying tensioning spring with help of “tension_tune.m’ included in appendix I.
- Generate the file containing drive-off motion.
- Run RIFLEX analysis with implemented drive-off motion.

3.5 Weak Link

The objective for the weak link analysis is to investigate the dynamic response of a riser during the event of a weak link fracture. A weak link fracture would result in release of potential energy stored in the tensioning system and as elastic strain in the riser. An additional effect is the release of the highly pressurized content of the riser into the environment. The presented work does not account for the latter phenomenon, since it is a very complex effect which would require multi disciplinary work and therefore is out of the scope of the thesis.

Both the weak link model and the deep water drive-off model have the same base. Some modifications were performed in order to simulate weak-link fracture. The lower parts (WH,XT,EDP, LRP) was removed, and the lower end of the riser pinned. The reason for the modification is that disconnection of nodes in between

lines is difficult (perhaps not possible) in the RIFLEX version used for the analysis. The weak link is located at the pinned lower end. Components below the weak link is not accounted for, but it is reasonable to assume that these components does not affect the response in a noticeable manner.

The lower end of the riser is tracked in the time domain in order to give an impression of the response following the fracture. Results are intended to be used to investigate whether is feasible to install a limiting device that increases the tangential drag of the riser at the lower end in order to reduce the impact of a weak-link failure. Several analyses were performed where the tangential drag coefficient for a unit area at the lower end was increased. Results are presented as a plot of the drag coefficient versus the maximum vertical response.

Note that this approach only accounts for the increase in tangential drag force. If a components is to be installed at the lower end it would also contribute with added mass, extra mass and normal drag.

3.5.1 Tangential drag

The length of the line used for parametric variation of drag is calculated based on equation 3.4. Length of the line used for parametric study was calculated so that the area of the line equals to one. It should make it fairly simple to compare the results with the drag of another object.

$$F_{D_t} = \frac{1}{2} C_D \rho_{sw} \pi D L v^2 \quad (3.4)$$

Where:

F_{D_t} is the tangential drag force.

C_D is the tangential drag coefficient.

D is the outer diameter of the riser.

L is the length of the segment.

v is the tangential velocity.

ρ_{sw} is the density of seawater.

3.5.2 Analysis methodology

The first step of the weak link analysis is to tension the system to the point where a weak link fracture would occur. In the presented work it is assumed that the weak link is designed to break at 460 tonnes of tension. This is based on information

provided by AKSO and should represents a realistic value. The offset at which the fracture load is obtained was established by parametric variation using STAMOD the plot showing static offset vs tension at weak link is found in figure 3.12. From the figure it is seen that a vessel offset of 330[m] should be sufficient to provide the required tension.

Following the static analysis a dynamic analysis that displaces the vessel into position and simulates the weak link fracture was performed. In order to ensure that any dynamic effects have passed, the axial force was plotted in the time domain. Figure 3.13 shows that the dynamic effects from the offset had worn off before the boundary condition change at 600 [s]. Figure 3.14 shows the vertical position of the lower riser end during the analysis. The parametric study is based on plotting the maximum amplitude of the lower end for different axial drag coefficients.

A brief summary of the steps is presented below:

1. Static parameter variation to establish offset with desired tension at weak link.
2. Dynamic analysis where axial force is monitored to ensure correct tension.
3. Batch run of dynamic analysis where the drag of the lower end is increased.

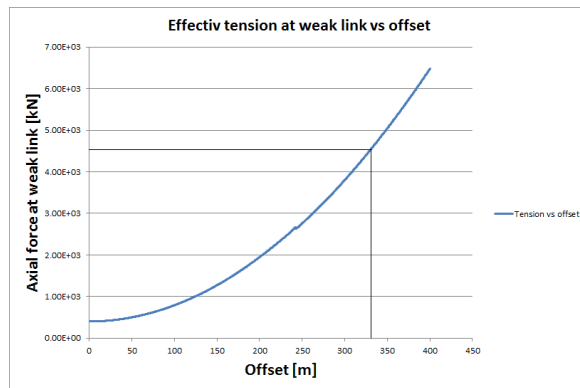


Figure 3.12: Effective tension at the weak link versus vessel offset.

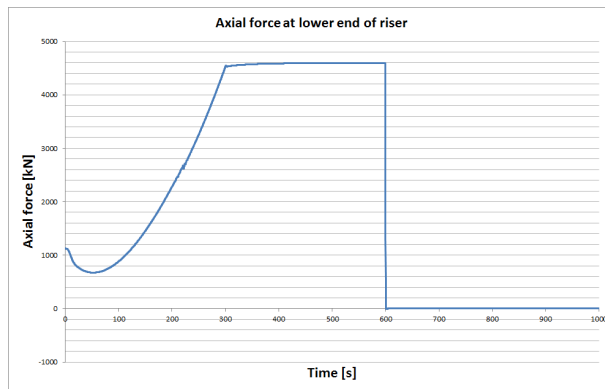


Figure 3.13: Effective tension at the weak link versus vessel offset.

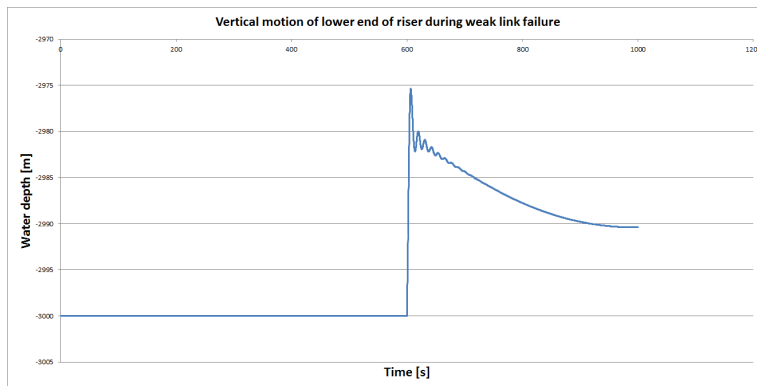


Figure 3.14: Time series of lower end vertical movement

3.5.3 Parametric variation

3.5.4 Reflex model

The reflex model is based on the deep water drive-off model. In order to perform the drag coefficient parameter study, a line with unit area and standard riser profile was added under the TSJ. Figure 3.15 gives an overview of the weak link model.

- Supernode
- ▬ Standard riser with extra buoyancy

○ Line number

▬ Standard riser

Emodulus: 205 [GPa]

Standard riser:

OD 0.2445 [m]
 ID 0.1930 [m]
 Density 7850 [kg/m³]

Buoyancy module:

t_{ext} 0.2 [m]
 Density 400 [kg/m³]

TSJ:

OD - Start 0.2350 [m]
 OD - End 0.2650 [m]
 ID - Start 0.1842 [m]
 ID - End 0.1842 [m]
 Density 7850 [kg/m³]

6 x PIP Heave compensator cylinders

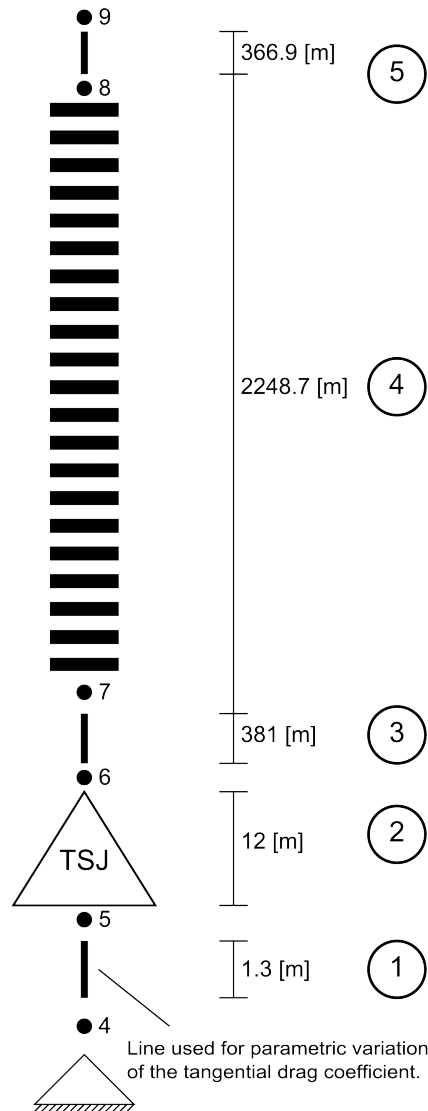


Figure 3.15: Model used for weak link analysis.

Chapter 4

Results

4.1 Drive-off

4.1.1 Riser snapshots

In this section a selection of snapshots of the riser during the analyses is presented. The illustrations show how the riser behaves during the drive-off. Riser position at vessel maximum offset is marked with green, the riser during drive-off is marked with blue and during return the riser is marked red. Time snapshots are included in order to give a better impression of the dynamic behaviour of the system as a whole. Riser time snapshots are presented for a representative selection of the cases investigated. Snapshots of the case with uniform current is not included since the deep water configuration did not converge due to the high loads.

Figure 4.1 shows time snapshots of the deep water riser during downstream drive-off with and without return. No current is active. It is easy to see that it is a significant delay between floater movement and riser response. Observe that the vessel returns long before the riser is any where near reaching static equilibrium, and that it is a significant difference between the maximum x-position along the riser for drive-off to static offset compared with the case including return.

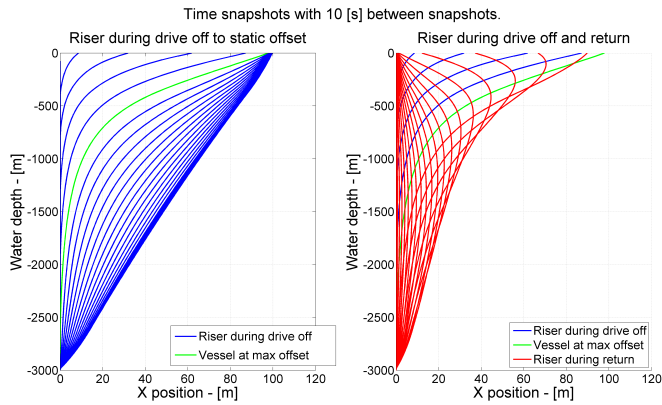


Figure 4.1: Deep water time snapshots, 50 [s] 100[m] drive-off no current.

Figure 4.2 displays the shallow water riser during downstream drive-off with no current. The riser does not show significant time delays and the riser closely follows the vessel motion. Meaning that the lower angle for the shallow water cases can be expected to be closely linked to the vessels position.

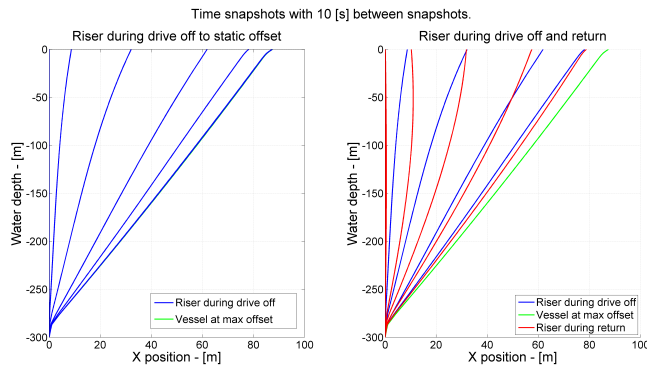


Figure 4.2: Shallow water time snapshots, 50 [s] 100[m] downstream drive-off no current.

When introducing shear current to the deep water riser as shown in figure 4.3 and figure 4.4, the riser seems to respond quicker compared with the case with no current. Take note of the large initial deflection due to the current.

Figure 4.3 displays the deep water riser during downstream drive-off. Note how the upper part of the riser assumes an “S” shape when the vessel moves. The “S” shape occurs as a result of the large drag on the upper parts of the riser. The part of the riser with the highest curvature moves down the riser compared to the case

without current.

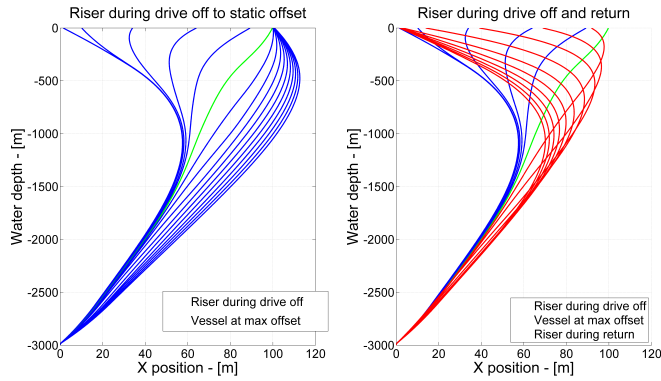


Figure 4.3: Deep water time snapshots, 50 [s] 100[m] downstream drive-off shear current.

Figure 4.4 displays the riser with a shear current during an upstream drive-off. The large drag causes the riser to move slower, and it takes a long time before static equilibrium is reached.

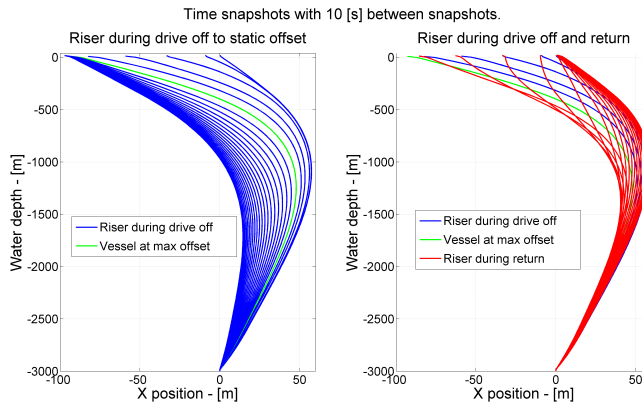


Figure 4.4: Deep water time snapshots, 50 [s] 100[m] upstream drive-off shear current.

Introduction of shear current does not seem to alter the shallow water riser behaviour significantly. A slightly higher curvature is observable during the return motion.

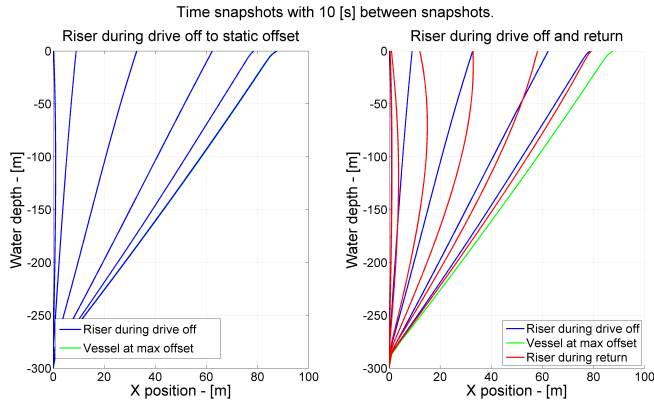


Figure 4.5: Shallow water time snapshots, 50 [s] 100[m] drive-off shear current.

4.1.2 Lower angle of the riser

The riser snapshots give an impression of how the riser behaves during the simulation, but provides little quantitative information. In order to investigate the effect of drive-off on riser disconnect, monitoring of the lower angle of the riser is of importance. Lower angles are calculated as described in section 3.2. Positive angles means downstream rotation, negative angles means upstream rotation. In all cases the vessel motion starts at 50[s] and reaches its maximum amplitude at ± 100 [m] at 100[s].

In the following the lower angle for the various cases is presented. By comparing shallow versus deep water, and upstream versus downstream results, critical cases can be identified and dynamic behaviour observed. Remember that the presented lower angle is the relative angle between the wellhead and the TSJ. Return motion is simulated by reversing the offset motion unless otherwise is stated. A study investigating the effect of return motion for the deepwater riser is presented. Finally a rerun displaying results for deep water upstream simulations with an improved model is shown.

Figure 4.6 and figure 4.7 displays the shallow water results for upstream and downstream drive-off.

Both up and downstream simulations show the same tendencies, the angles for shallow water configuration are closely related to the vessel offset. For the downstream drive-off the cases with uniform current is the critical, while for upstream drive-off the cases without current reveals the largest angles. This shows that upstream drive-off is less critical with respect to the lower angle of the riser since the current helps reducing the angle with upstream offset and increasing it during downstream offset.

Different current cases have different initial angles due to drag. Both figures show some odd behaviour with high frequency response around 70-90[s] and after 150[s]. This behaviour is caused by the compression spring in the heave compensation system, as the simulations in section 4.1.2 reveals.

Large sensitivity with respect to vessel position is observed. Angles close to 8[degrees] which is far beyond critical values are not surprising since the maximum vessel offset is 1/3 of the water depth.

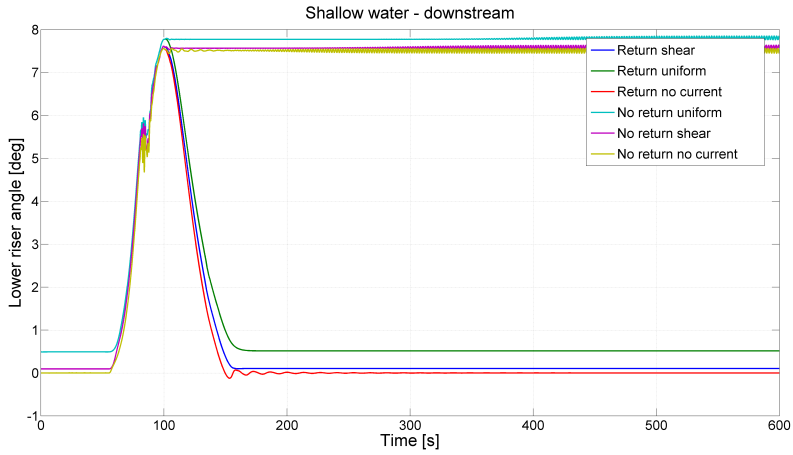


Figure 4.6: Lower angle during downstream drive-off with shallow water configuration.

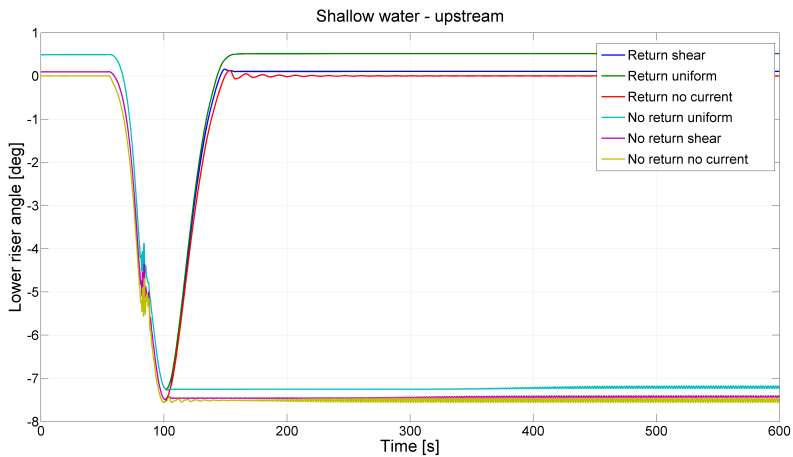


Figure 4.7: Lower angle during upstream drive-off with shallow water configuration.

The deep water up and downstream results are presented in figure 4.8 and figure 4.9. Deep water simulations show less direct relation between vessel position and lower angle, there is more dynamic in play.

Figure 4.8 shows the lower angle of the downstream deep water simulations. The shear current simulations show an initial dip of the lower angle around 50-80[s]. The effect is caused by loss of tension during the initial drive-off as a result of the high drag on the upper parts of the riser.

It is interesting to note that the angle increases faster and have a lower maxima for cases with return and current. The lower angles for the deep water simulations does not reach critical values for any of the cases simulated.

A simple comparison with a right-angled triangle with sides equal to 100[m] and 3000[m] means that an maximum expected angle should be around 1.9 [deg]. The maximum angle observed is in the case of no return shear, and equals around 1.38[deg] some what lower than the simple estimate.

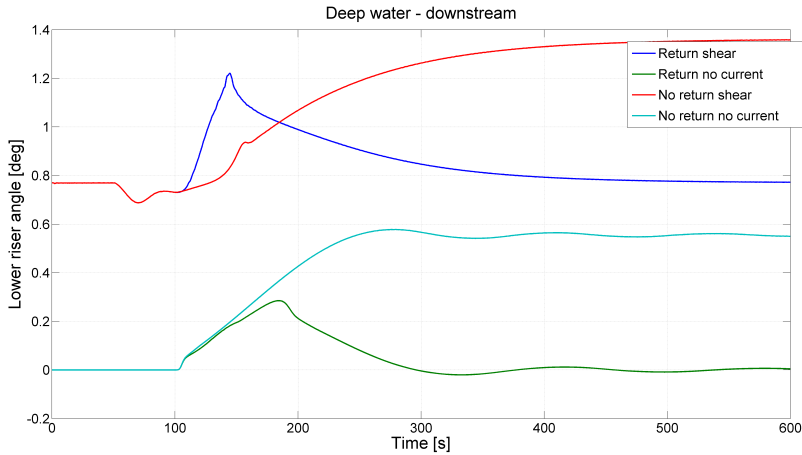


Figure 4.8: Lower angle during downstream drive-off with deep water configuration.

The deep water upstream drive-off results are summarized in figure 4.9. Note that the lower angle behaves quite non-intuitive from around 50 [s] to around 80 [s] for the cases with shear current. The increase in angle is caused by the large drag on the upper parts of the riser, increasing the tension in the riser and thereby increasing the lower angle before the vessel offset reduces it. Around 70 - 80 [s] a high frequency noise is observed, it is caused by the high loads resulting in numerical difficulties with the compression spring in the PIP heave compensator.

For the case without current a reduction in the riser angle is observed after a delay of around 55 [s].

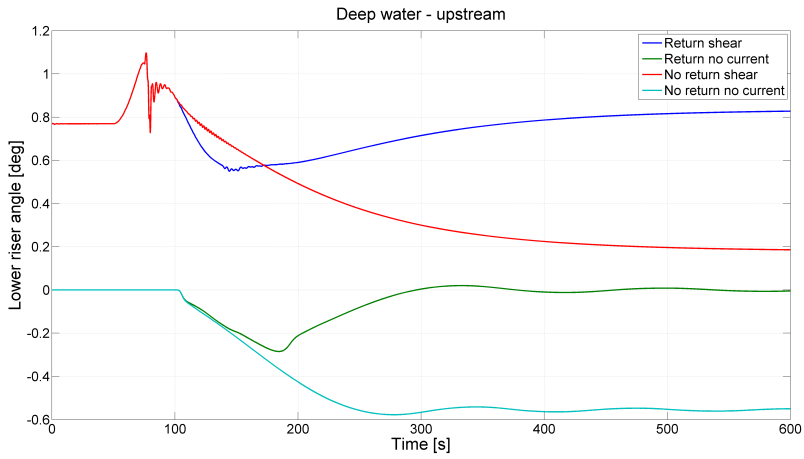


Figure 4.9: Lower angle during upstream drive-off with deep water configuration.

Figure 4.10 illustrates how the lower angle increases faster with return motion implemented for the downstream drive-off. This is interesting and may indicate that the vessels returning motion can play a critical role in reducing maximum angle when returning from a drive-off.

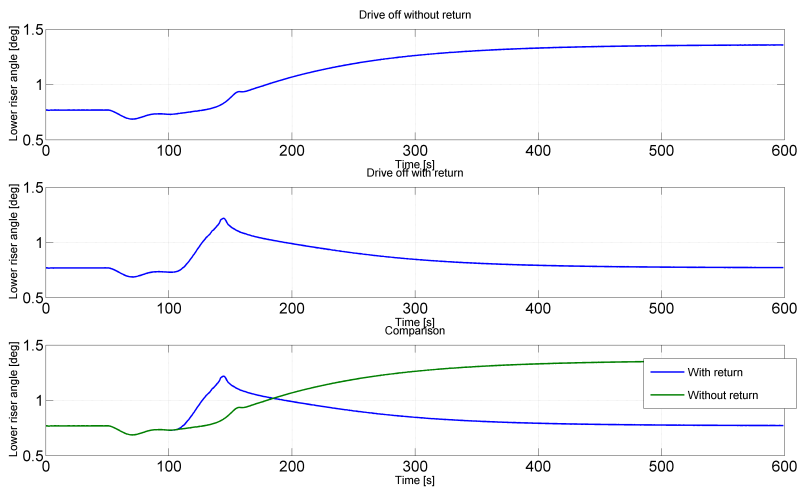


Figure 4.10: Deep water lower angle comparison during downstream drive-off to 100[m] offset in 50 [s].

Effect of vessel return motion

The effect of vessel return was studied for the deep water shear current. The return motion was modelled as described in chapter 3.4.2. The intention of this study is to identify how the vessels return motion affects the lower angle and if the maximum angle can be reduced by controlling the vessels return motion.

Figure 4.11 displays the results of the downstream study with altered return motion. Lower angle increases faster with shorter return durations. Return duration affects the angle amplitude, and a non significant 0.05 [deg] difference is observed between the 75 [s] return and the 200 [s] return. The difference in amplitude may be larger for larger vessel offsets. The 25 [s] case shows some of the same issues that was observed in the upstream and shallow water drive-off simulations where high frequency noise is introduced in the system.

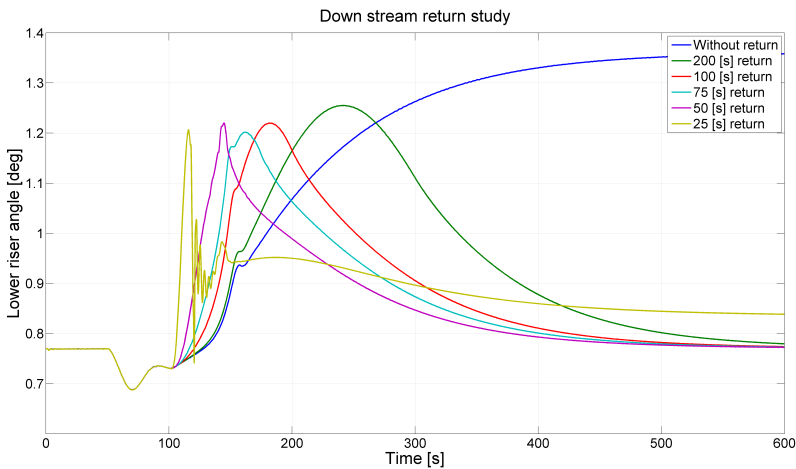


Figure 4.11: Study of return motion on deep water riser with downstream vessel motion.

In figure 4.12 the results of the upstream study is presented. The results contain noise due to the high loads. A relation between maximum amplitude and return motion is more pronounced for these results than for the downstream simulations. On the other hand the angle amplitudes are much lower than the static solution, again showing that upstream drive-off is less critical than downstream with respect to riser angles.

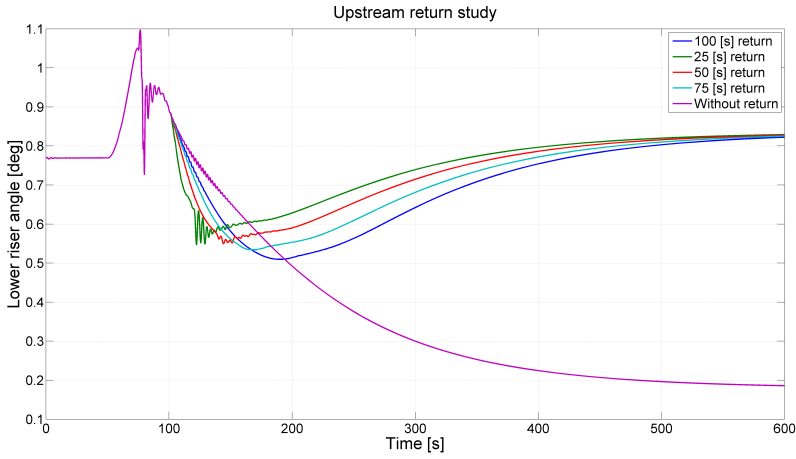


Figure 4.12: Study of return motion on deep water riser with upstream vessel motion.

Upstream deep water with tension spring

Due to the high amounts of noise in the results for the upstream deep water analysis, a rerun with a tension springs was in place. The rerun will also help to identify if the noise in the other results is caused by numerical issues with the compression of the tensioner springs.

As seen in figure 4.13 most of the noise is gone when simulating with a tension spring. It was even possible to perform analysis on the uniform current case. For further studies it is therefore recommended to use the tensioned spring model.

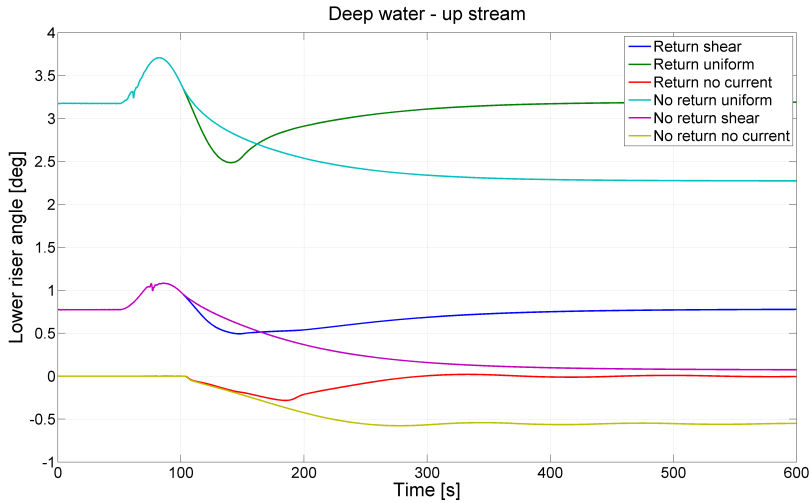


Figure 4.13: Lower angle during upstream drive-off with deep water configuration using the tensioned spring model.

4.2 Weak link fracture

The weak link fracture simulations was performed as described in chapter 3.5. Figure 4.14 displays the motion in three directions for the lower end of the riser. Motion in the Y direction is equal to zero as expected. A pendulum motion caused by current can be observed as a large offset in the x-direction.. This motion is part of the reason why the vertical position converges towards higher value.

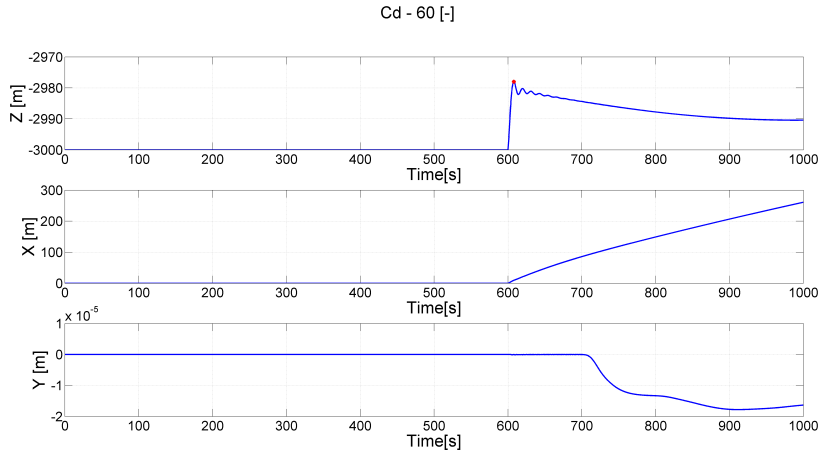


Figure 4.14: Motion of the lower end of the riser after weak link fracture.

A parametric study was performed where the tangential drag coefficient of the unit area at the lower end of the riser was increased from 0 to 600 with increments of 10. The results show that the effect of the increasing tangential drag decreases rapidly as a result of reduced velocities. The parametric study shown in figure 4.15 reveal that the drag have to be significantly increased in order to reduce the vertical response. Note that this study does not account for added mass, and mass of a device installed to reduced the response.

The mass and added mass can make a significant difference in the results, since the peak accelerations are very high as figure 4.16, and figure 4.17 illustrates. The difference in velocity for the case of zero tangential drag compared with a cd of 600 [-] is easily seen. Be aware that the velocities and accelerations in the two figures are derived from the displacements, the data points are not sufficient for representation of the acceleration peak.

Figure 4.18 reveals that the acceleration peaks are represented by a single data point. The data set has a time incrementation as low as 0.04[s] meaning that extra care should be taken when selecting time incrementation for weak link fracture simulations. It is important that the incrementation is selected so that acceleration, velocity and displacement is properly represented. Running weak-link fracture with very small time incrementation can be very time consuming. In order to reduce time consumption utilization of the restart functionality in RIFLEX can be a good option. Using a large time increment in the time before fracture, reducing it before fracture so that the response can be properly simulated.

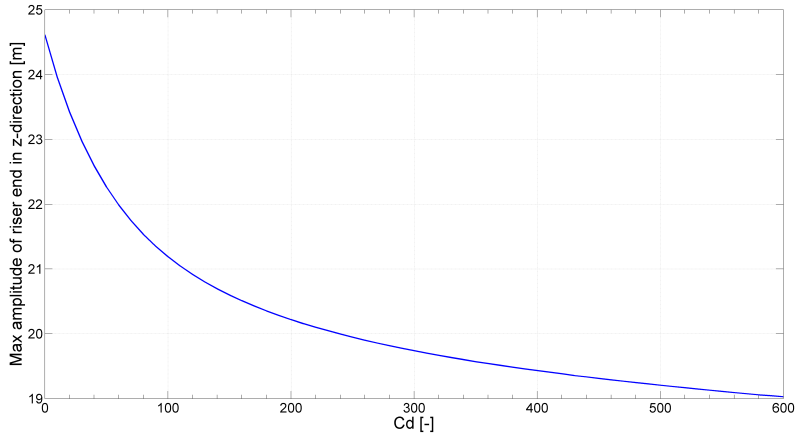
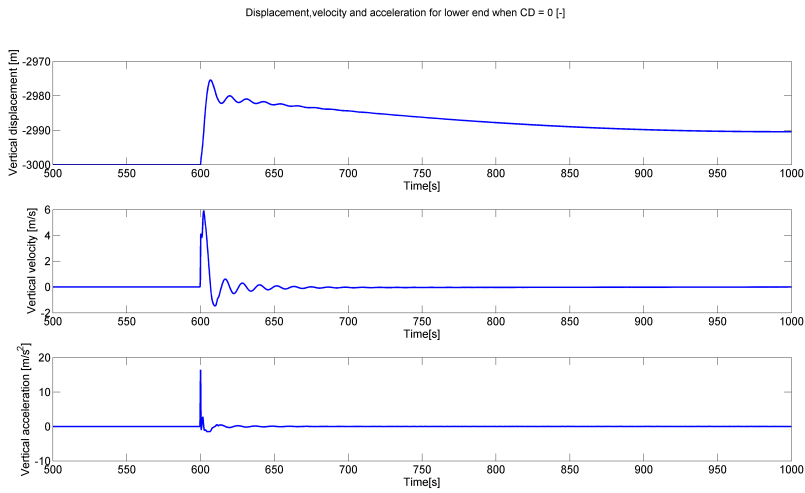


Figure 4.15: Parameter study of weak link fracture.

Figure 4.16: Vertical displacement, velocity and acceleration for lower end, $cd = 0$

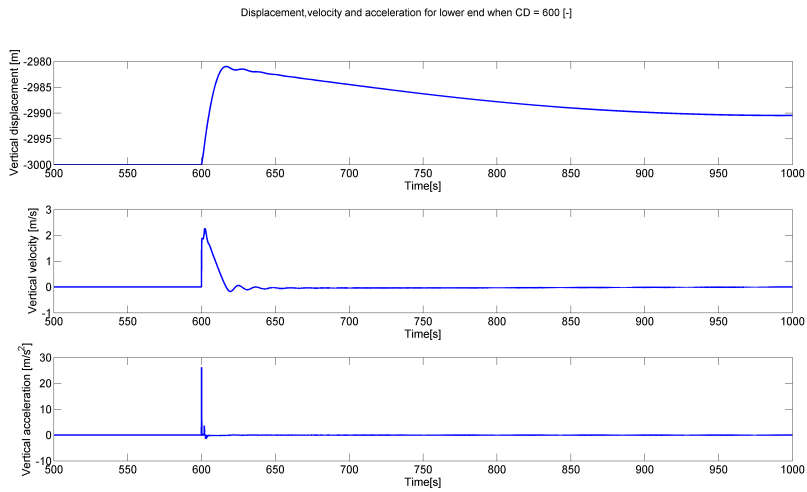


Figure 4.17: Vertical displacement, velocity and acceleration for lower end, $cd = 600$

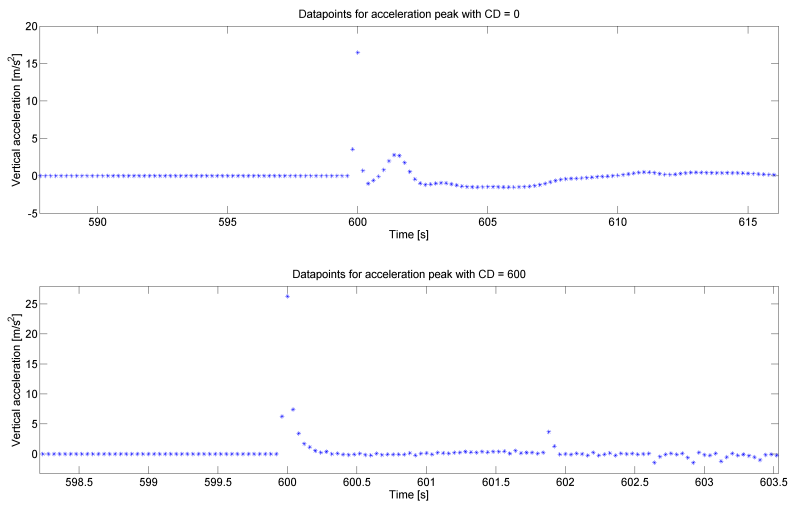


Figure 4.18: Data points for vertical acceleration.

Chapter 5

Conclusion

Drive-off scenarios including return, and weak-link fracture have been investigated in this work. Main effort has been on modelling aspects and dynamic effects. Several cases of drive-off with and without return were investigated. A parametric study of a weak link fracture occurring at 460 tonnes of over pull was performed. Models using pipe-in-pipe contact formulation were implemented in the simulations.

The drive-off simulations revealed a close link between vessel position and lower riser angle for the shallow water simulations. Deep water simulations showed a much more dynamic picture, including delays in response, initial effects and rapidly increasing angles when including return motion.

As mentioned monitoring lower riser angle during drive-off showed delays of around 60[s] before the riser responded with rotation in the vessel offset direction. When including current, an initial effect during drive-off, rotating the lower end of the riser away from the vessel was observed. The effect is a result of the high drag on the upper parts of the riser, increasing the riser tension for upstream drive-off and reducing it for downstream drive-off. When comparing the upstream versus the downstream simulations, it was clear that the current reduced the maximum angle for the upstream simulations and increased it for downstream simulations.

When establishing drive-off watch circles, one should consider the effect of current, and evaluate the possibilities for taking advantage of the time delay on deep water systems.

Adding a return motion to the vessel resulted in a faster increase of the riser angle for cases including current. Variation of return motion did not significantly affect the maximum lower angle, but had impact on the angles rate of change. This means that taking advantage of the time delay when establishing operational envelopes may be difficult since the maximum amplitude were close to the static offset levels during return. However this study only included a vessel offset of 100[m], the

picture might change for larger offsets.

Upstream simulations revealed some weaknesses in the initial modelling of the heave compensation system causing noise in the results. Some of the simulations was rerun with an improved model which demonstrated that the noise was caused by the compression of the springs in the heave compensation system.

Weak link fracture required a model capable of representing the heave compensation system after release of the lower riser end. The pipe-in-pipe model was selected since it had the required specifications. High riser tension during weak link simulations revealed numerical issues with the PIP model, causing the analyses to fail due to large rotations in the heave compensator springs. The issue was solved by modifying the spring representing the pressure banks of the compensation system. Basically the springs was rearranged in a way so they would be tensioned instead of compressed. The modification resulted in a large improvement in numerical stability and reduced analysis run time significantly. A drawback of the modification is that it does not allow correct force and moment representation for the heave compensator. An improved model adding springs and slave nodes ensuring conservancy the force and moment representation was proposed.

Simulations showed a large vertical displacement of 24.5[m] following the weak link fracture. Parametric studies revealed that the amplitude of the motion could be reduced by around 5[m] by significantly increasing the lower end drag. The results does not account for increase in added mass and mass of an installed device limiting weak link response. Large acceleration peaks following the fracture indicates that mass and added mass may have a significant influence on the response. Special care should be taken with respect to the time incrementation to ensure a correct representation of the seconds after fracture. For instance by making use of the restart functionality in RIFLEX.

Hopefully these findings can prove useful for further studies on drive-off and weak link fracture.

Chapter 6

Further work

To fully understand drive-off and weak link events there is still work to be done. In the following further work based on the findings in the thesis is suggested.

The suggested PIP model with extra springs and slave nodes should be tested and verified.

6.1 Drive-off

The following list summarized the improvements

- The drive-off simulations should be rerun and verified with the improved model of the tension system.
- Comparison between drive-off model with PIP and with simpler modelling.
- Identify suitable analysis tools to run coupled analysis where the angle between riser and vessel can be properly studied.
- Investigate the combination of drive-off with return on deep water scenarios with larger drive-off amplitudes.

6.2 Weak link fracture

- Study to identify possible devices that can limit response and their hydrodynamic properties and mass.
- Estimate and include the “rocket” effect that occurs when releasing the high pressure content of the riser.

- Investigate possibility of a model including the response on the topside, making it easier to evaluate risk for personel.
- Implement restart functionality to shorten analysis run time and increase accuracy in the time after fracture.

Bibliography

- [Rif, 2010] (2010). *Riflex User Manual v 3.6 rev8*.
- [mat, 2011] (2011). <http://www.mathworks.com/matlabcentral/fileexchange/18909-replace-strings-in-text-file>.
- [Brynestad, 2011] Brynestad, B. I. (2011). Analysis of workover risers on very deep water.
- [Ervik, 2011] Ervik, A. K. (2011). Analysis and monitoring of drilling risers on dp vessels.
- [Faltinsen, 1990] Faltinsen, O. M. (1990). *Sea loads on ships and offshore structures*. Cambridge university press.
- [Langen and Sigbjörnsson, 1979] Langen, I. and Sigbjörnsson, R. (1979). *Dynamisk analyse av konstruksjoner*.
- [Rustad et al., 2012] Rustad, A. M., Ervik, A. K., Sørensen, A. J., and Larsen, C. M. (2012). Increasing the operation window for drilling risers on dp vessels by monitoring riser angles. In *OMAE 2012*.

Appendix A

Matlab script for calculation of global angle

```
1 function [ theta ] = globang( n1,n2 )
2 %Calculates the angle between a line defined by two points and the ...
   z-axis
3 %
4
5 theta = atan((n2(:,1)-n1(:,1))./(n2(:,2)-n1(:,2)))*180/pi;
6 end
```

Appendix B

Matlab script for calculation of relative angle

```
1 function [ theta ] = relang( n1,n2,n3 )
2 %RELANG Calculates the relative angle from -90 to 90 degrees between
3 %two lines connected by three points.
4 % n1 - Vector containing coordinates of lower node.
5 % n2 - Vector containing coordinates of middle node.
6 % n3 - Vector containing coordinates of top node.
7 % theta - relative angle between lines
8 % theta1 - angle between x-axis and line one
9 % theta2 - angle between z-axis and line two
10
11 theta1 = atan( (n2(:,1)-n1(:,1))./(n2(:,2)-n1(:,2)));
12 theta2 = atan( (n2(:,1)-n3(:,1))./(n2(:,2)-n3(:,2)));
13
14 theta = (theta2-theta1)*180/pi;
15
16 end
```

Appendix C

geninp.m

```
1 function [ out casenames varnames vars] = geninp( inpdr ,inp, ...
   temdr, tem )
2 %GENINP Generates folder structures where variables in a template file
3 %   are replaced according to the inputfile.
4 %
5 % The input file should be a textfile formatted as shown between ...
   the dashed lines
6 % below. There are no limitations to how many variables or cases ...
   that can be
7 % included.
8 %
9 % example.inp
10 % ...
-----
11 %   Cases   Var1   Var2   Var3
12 %   Case1   -     -     -
13 %   Case2   -     -     -
14 %   Case3   -     -     -
15 %   ...
-----
16 % The spots marked with - should be replaced by the variable value ...
   corresponding
17 % to the relevant case. (Note: Variables should be numbers, and ...
   columns should be
18 % separated by tabulators.) Folders will be named after the cases. ...
   Variables
19 % wich are to be replaced have to have the same name in the input and
20 % template file.
21 %
22 % Input
23 %   inpdr   - directory for the inputfile.
24 %   inp     - name of the input file.
25 %   temdr   - directory for the template file.
26 %   tem     - name of the template file.
27 %
28 % Output
```



```
29 %         out   - returns true if the process completed.
30 %
31 %
32 % Author: Benjamin I. Brynestad - 08.02.2012
33
34 out = false;
35 inpath = [inpdr '\\' inp];
36 tempath = [temdr '\\' tem];
37
38 if isempty(inpdr) || isempty(inp) || isempty(temdr) || isempty(tem)
39     return
40 elseif ~ischar(inpdr) || ~ischar(inp) || ~ischar(temdr) || ~ischar(tem)
41     return
42 end
43
44 data = importdata(inpath);
45
46
47 vars = data.data;
48
49 ncases = size(vars,1);
50 nvars = length(data.textdata(1,:)) - 1;
51
52 casenames = data.textdata([2:ncases+1],1);
53 varnames = data.textdata(1,[2:nvars+1]);
54
55 for i = 1:ncases
56     %Create a folder for the relevant case
57     mkdir(temdr,char(casenames(i)));
58     %Copy the template to the folder
59     copyfile(tempath,[temdr '\\' char(casenames(i))]);
60     %Storing current file path
61     currpath = [temdr '\\' char(casenames(i))];
62
63     for j = 1:nvars
64
65         replaceinfile(char(varnames(j)), num2str(vars(i,j)), ...
66             [currpath '\\' tem], '-nobak');
67     end
68 end
69 out = true;
70 end
```

Appendix D

riflex__test.m

```
1 function res = riflex_test(dr,pref1,pref2)
2 %UNTITLED3 Summary of this function goes here
3 % Detailed explanation goes here
4
5
6 bat = 'C:\SINTEF\riflex_3_7_24\etc\riflex.bat';
7 %bat = 'C:\Marintek\MSE\Riflex\etc\riflex.bat';
8
9 curdir = cd; % remember old directory
10 cd(dr); % and move to the directory where it happens
11
12 tstart = tic;
13
14 cmd = [bat ' inpmod ' pref1 ];
15 status = dos(cmd, '-echo'); assert(~status, 'DOS reported an error');
16
17 cmd = [bat ' stamod ' pref1 ];
18 status = dos(cmd, '-echo'); assert(~status, 'DOS reported an error');
19
20 cmd = [bat ' dynmod ' pref2 ];
21 status = dos(cmd, '-echo'); assert(~status, 'DOS reported an error');
22
23 cmd = [bat ' outmod ' pref1 ' ' pref2];
24 status = dos(cmd, '-echo'); assert(~status, 'DOS reported an error');
25
26 cd(curdir);
27
28 tend = toc(tstart);
29
30 disp(['Duration of analysis: ' num2str(round(tend/60)) ' minutes']);
31 disp(['Analysis finished at: ' num2str(datestr(clock))]);
32 end
```

Appendix E

replaceinfile.m

```
1 function [s, msg] = replaceinfile(str1, str2, infile, outfile)
2 %REPLACEINFILE replaces characters in ASCII file using PERL
3 %
4 % [s, msg] = replaceinfile(str1, str2, infile)
5 %   replaces str1 with str2 in infile, original file is saved as ...
   "infile.bak"
6 %
7 % [s, msg] = replaceinfile(str1, str2, infile, outfile)
8 %   writes contents of infile to outfile, str1 replaced with str2
9 %   NOTE! if outfile is '-nobak' the backup file will be deleted
10 %
11 % [s, msg] = replaceinfile(str1, str2)
12 %   opens gui for the infile, replaces str1 with str2 in infile, ...
   original file is saved as "infile.bak"
13 %
14 % in:  str1      string to be replaced
15 %      str2      string to replace with
16 %      infile    file to search in
17 %      outfile   outfile (optional) if '-nobak'
18 %
19 % out: s         status information, 0 if succesful
20 %      msg       messages from calling PERL
21
22 % Pekka Kumpulainen 30.08.2000
23 % 16.11.2008 fixed for paths having whitespaces,
24 % 16.11.2008 dos rename replaced by "movefile" to force overwrite
25 % 08.01.2009 '-nobak' option to remove backup file, fixed help a ...
   little..
26 %
27 % TAMPERE UNIVERSITY OF TECHNOLOGY
28 % Measurement and Information Technology
29 % www.mit.tut.fi
30
31 message = nargchk(2,4,nargin);
32 if ~isempty(message)
33     error(message)
```

```
34 end
35
36 %% check inputs
37 if ~(ischar(str1) && ischar(str2))
38     error('Invalid string arguments.')
39 end
40 % in case of single characters, escape special characters
41 % (at least some of them)
42 switch str1
43     case {'\ ' '.'}
44         str1 = ['\ ' str1];
45 end
46
47 %% uigetfile if none given
48 if nargin < 3;
49     [fn, fpath] = uigetfile('*. *', 'Select file');
50     if ~ischar(fn)
51         return
52     end
53     infile = fullfile(fpath, fn);
54 end
55
56 %% The PERL stuff
57 perlCmd = sprintf('%s', fullfile(matlabroot, ...
58     'sys\perl\win32\bin\perl'));
59 perlstr = sprintf('%s -i.bak -pe"s/%s/%s/g" "%s"', perlCmd, str1, ...
60     str2, infile);
61
62 [s, msg] = dos(perlstr);
63
64 %% rename files if outputfile given
65 if ~isempty(msg)
66     error(msg)
67 else
68     if nargin > 3 % rename files
69         if strcmp('-nobak', outfile)
70             delete(sprintf('%s.bak', infile));
71         else
72             movefile(infile, outfile);
73             movefile(sprintf('%s.bak', infile), infile);
74         end
75     end
76 end
77 end
```

Appendix F

Matlab functions used for post processing drive off

```
1 function post_process( mat_path, finish_dir, analysis_type, ...
    prefix, varargin)
2 %POST_PROCESS Starts the processing of data from .mat files based on
3 %analysis type
4 %
5 %   Input: mat_path      - String containing the path to the .mat ...
    file containing
6 %
    time series data.
7 %   finish_dir    - Directory where post processes results ...
    should be
8 %
    placed.
9 %   analysis_type - String describing the type of analysis.
10 %   prefix       - Prefix used to name output
11 %
12 %   Recognised analysis types:  D_NR - Drive off to static offset need
13 %
    additional input of colum number
14 %
    containing data for
15 %
    the nodes used in angle
16 %
    calculations. Format is [x1 ...
17 %
    z1], [x2
18 %
    z2], [x3 z3]. Where 1 ...
19 %
    corresponds to
20 %
    the lower node and 3 to the top
21 %
    node. In addition the ...
22 %
    amplitude and
23 %
    duration untill max ...
24 %
    amplitude should
25 %
    be inculded.
    D_R - Drive off returning to original
    position
26 % Benjamin I. Brynestad - 2012
```

*APPENDIX F. MATLAB FUNCTIONS USED FOR POST PROCESSING
DRIVE OFF*

```
26
27 if strcmp(analysis_type , 'D_NR')
28     % varargin{1} - row number s for lower node
29     %         2 - middle
30     %         3 - top
31     %         4 - Duration of drive off
32     %         5 - Amplitude of drive off
33     %         6 - Time incrementation used in dynamic analysis.
34     post_drift_nr(mat_path, finish_dir, varargin{1}, varargin{2}, ...
35                 varargin{3}, prefix, varargin{4}, varargin{5},varargin{6});
36 elseif strcmp(analysis_type, 'D_R')
37     post_drift_nr(mat_path, finish_dir, varargin{1}, varargin{2}, ...
38                 varargin{3}, prefix, varargin{4}, varargin{5},varargin{6});
39 else
40     error('Analysis type not recognised.')
```

```
1 function post_drift_nr( mat_path, out_dir,n1,n2,n3, prefix, ...
2     dur,amp, dt_sim)
3 %POST_DRIFT_NR postprocesses timeseries data from .mat files.
4 %
5 % Input: mat_path - String containing the path to the .mat file.
6 % out_dir - Directory where post processes results are stored.
7 % n1 - Lower node coulumn number.
8 % n2 - Middle node coulumn number.
9 % n3 - Top node coulumn number.
10 % prefix - String used to name the output.
11 % dur - Duration untill max amplitude of drive off.
12 % dt_sim - Time incrementation used in the dynamic analysis
13 % Benjamin I. Brynstad - 2012
14
15 riser_time = importdata(mat_path);
16 t_end = size(riser_time,1);
17 t_inc = 10;
18 t = riser_time(1:t_inc:t_end,1);
19
20 lower_angle = relang(riser_time(1:t_inc:t_end,n1), ...
21                     riser_time(1:t_inc:t_end,n2), riser_time(1:t_inc:t_end,n3));
22 lower_angle_glob = ...
23     globang(riser_time(1:t_inc:t_end,n2),riser_time(1:t_inc:t_end,n3));
24
25 scrsz = get(0,'ScreenSize');
26 figure('OuterPosition',[1 scrsz(4)/2 scrsz(3)/2 scrsz(4)/2])
27
28 plot(t,lower_angle,'Linewidth',2);
29 hold on
30 plot(t,lower_angle_glob,'m','Linewidth',2);
31
32 [max_ang time] = max(lower_angle);
33 plot(t(time),max_ang,'*r');
34
35 try
36     plot(t((dur+50)/dt_sim/t_inc), ...
37         lower_angle((dur+50)/dt_sim/t_inc) , 'Ok', 'LineWidth',2)
38 end
```

*APPENDIX F. MATLAB FUNCTIONS USED FOR POST PROCESSING
DRIVE OFF*

```
34     legend('Lower angle - rel','Lower angle - glob','Max ...  
           angle','Drive off ending','Location','Best')  
35     xlabel('Time[s]')  
36     ylabel('Angle[deg]')  
37     title(['Drive-off: Amplitude - ' num2str(amp) ' m Duration of ...  
           driveoff - ' num2str(dur) ' s' ])  
38     set(gca,'LineWidth',1);  
39     grid on  
40  
41  
42     print(gcf, '-dpng',[out_dir '\\' prefix])  
43     close  
44  
45     end
```

Appendix G

Matlab function used to convert ascii files to mat

```
1 function convert_timeseries_to_mat(input_file,timeseries,path)
2 %input_file = 'No_waves_return.inp';
3 %timeseries = '206m_PIP_aller_mod_noddiss.asc';
4 %path = ...
5     'C:\Users\Benjamin\Documents\Master\Riflex\Driveoff\No_waves_return';
6 %path = cd;
7
8 data = importdata([path '\' input_file]);
9 mkdir([path '\Matlab_time_series'])
10
11 vars = data.data;
12
13 ncases = size(vars,1);
14 nvars = length(data.textdata(1,:)) - 1;
15
16 casenames = data.textdata([2:ncases+1],1);
17 varnames = data.textdata(1,[2:nvars+1]);
18 h = waitbar(0,'Converting acii files to mat:');
19
20
21 for i = 1:ncases
22     try
23
24         riser_time = importdata([path '\' char(casenames(i)) '\' ...
25             timeseries]);
26         save([path '\Matlab_time_series\' char(casenames(i)) ...
27             '.mat'],'riser_time')
28     catch
29         disp(['Could not post process data from ' path 'Case:' ...
30             char(casenames(i))])
31     end
32 end
```

*APPENDIX G. MATLAB FUNCTION USED TO CONVERT ASCII FILES TO
MAT*

```
29     waitbar(i/ncases,h)
30 end
```

Appendix H

Matlab functions used to generate drive off

Without return to start position

```
1 % Generates a file containing vessel positions along x-axis. For use
2 %           with drive off analysis with Reflex.
3 %
4 %
5 %
6 function ...
    offset_NO_return(drive_off_duration,drive_off_amplitude,base_dir)
7
8 simulation_time = 600;
9 time_increment = 0.1;
10 drive_off_start_time = 50;
11
12 t = time_increment:time_increment:simulation_time;
13 y(1:length(t)) = 0;
14 z(1:length(t)) = 0;
15 x = zeros(1,length(t));
16
17
18
19 for i = 1:length(t)
20
21     if t(i) > drive_off_start_time && t(i) <= (drive_off_start_time+ ...
22         drive_off_duration)
23
24         x(i) = drive_off_amplitude * sin(pi/2/drive_off_duration * ...
25             (t(i)-drive_off_start_time))^2;
26
27     else
28         try
29             x(i) = x(i-1);
30         end
31     end
32 end
```

```

28     end
29 end
30 %plot(t,x)
31 M = [t',-x',y',z'];
32 dlmwrite([base_dir '\' num2str(drive_off_duration) ...
          's_driveoff_to_' num2str(drive_off_amplitude) ...
          'm_NO_return.txt'], M, 'delimiter', '\t', ...
          'precision', 6);
33
34 end

```

Returning to start position

```

1  % Generates a file containing vessel positions along x-axis. For use
2  %                               with drive off analysis with Reflex.
3  %
4  %
5  %
6  function ...
    offset_return(drive_off_duration,drive_off_amplitude,base_dir,return_dur)
7
8  simulation_time = 600;
9  time_increment = 0.02;
10 drive_off_start_time = 50;
11
12 t = time_increment:time_increment:simulation_time;
13 y(1:length(t)) = 0;
14 z(1:length(t)) = 0;
15 x = zeros(1,length(t));
16
17 %Motion for return
18 %drive_off_duration = 2*drive_off_duration;
19
20 for i = 1:length(t)
21
22     if t(i) > drive_off_start_time && t(i) <= (drive_off_start_time+ ...
        drive_off_duration)
23
24         x(i) = drive_off_amplitude * sin(pi/2/drive_off_duration * ...
            (t(i)-drive_off_start_time))^2;
25
26     elseif t(i) > (drive_off_start_time+ drive_off_duration) && t(i) ...
        <= (drive_off_start_time+ drive_off_duration + return_dur)
27         x(i) = drive_off_amplitude * cos(pi/2/return_dur * ...
            (t(i)-(drive_off_start_time+drive_off_duration)))^2;
28     else
29         try
30             x(i) = x(i-1);
31         end
32     end
33 end
34 %plot(t,x)
35 M = [t',-x',y',z'];

```

APPENDIX H. MATLAB FUNCTIONS USED TO GENERATE DRIVE OFF

```
36 dlmwrite([base_dir '\' num2str(drive_off_duration) ...  
           's_driveoff_to_' num2str(drive_off_amplitude) 'm_' ...  
           num2str(return_dur) 's_return.txt'], M, 'delimiter', '\t', ...  
37         'precision', 6);  
38 end
```

Appendix I

Matlab function used to tune tension

```
1 function [ Spri ] = tension_tune( Sta_tens )
2 %TENSION_TUNE Summary of this function goes here
3 % Detailed explanation goes here
4
5 % Gradient of the spring (Calculated from input file supplied by RS)
6 % should be tuned to properly represent the tension system
7 Grad = 435000 ;
8 %-158750. -0.25
9 %-50000. 0.0
10 % 58750. 0.25
11 tens = Sta_tens/6; % Dividing total top tension with number of ...
    cylinders
12
13 Spri.Force = [Grad*-0.25-tens -tens Grad*+0.25-tens];
14 Spri.Elong = [-0.25 0 0.25];
15
16
17 end
```